ELSEVIER

Microelectronic Engineering 46 (1999) 93–96

MICROELECTRONIC ENGINEERING

$TiSi_xN_y$ and $TiSi_xO_yN_z$ as Embedded Materials for Attenuated Phase-Shifting Mask in 193 nm

Cheng-ming Lin and Wen-an Loong

Institute of Applied Chemistry, National Chiao Tung University, Hsin-Chu 300, Taiwan, Republic of China

$TiSi_xN_y$ and $TiSi_xO_yN_z$ were presented as new embedded materials for APSM in 193 nm lithography. $TiSi_xN_y$ films were formed by plasma sputtering of Ti (180~230 W) and Si (60~80 W) under Ar (50 sccm) and nitrogen (4~6 sccm). For required phase shift degree θ =180°, the calculated thickness d_{180} of $TiSi_xN_y$ film is 82~93 nm. $TiSi_xO_yN_z$ films were formed by plasma sputtering of Ti (200~240 W) and Si (60~80 W) under Ar (50 sccm), nitrogen (4~6 sccm) and oxygen (0.2~0.7 sccm). The d_{180} of $TiSi_xO_yN_z$ film is 92~105 nm. With the thickness d_{180}, the transmittance at visible wavelength (488, 632.8 nm) for optical alignment is 35~50% for $TiSi_xN_y$ and $TiSi_xO_yN_z$. Under BCl_3:Cl_2=14:70 sccm; chamber pressure 4 mtorr and RF power 1900 W, the dry etching selectivity of $TiSi_xN_y$ over DQN positive resist and fused silica, were found to be 2:1 and 4.8:1, respectively. A $TiSi_xN_y$ embedded layer with 0.6 μm lines/space was successfully patterned.

1. Introduction

Many embedded materials for AttPSM in 193 nm have been reported and also showed their drawbacks [1-4]. For example, the transmittance T% of Cr-F based materials at visible wavelength was found to be greater than 60%, too high for optical alignment. The Si-N based materials showed a low electric conductivity, would build up charging effect during e-beam direct-write. The Zr-Si based materials indicated that the reflectance R% in 193 nm wavelength is larger than 25%, too high to obtain a good resolution.

We have reported several Ti-based materials as new embedded materials for AttPSM [5-7]. In this paper, $TiSi_xN_y$ and $TiSi_xO_yN_z$ as new embedded materials suitable for AttPSM in 193 nm were presented. The two embedded materials were deposited by plasma sputtering of Ti and Si under argon and small amount of oxygen or nitrogen. A 0.6 μm line/space pattern using $TiSi_xN_y$ as embedded layer on SiO_2/Si substrate was successfully fabricated.

2. Experimental

$TiSi_xN_y$ films were formed by plasma sputtering of Ti (180~230 W) and Si (60~80 W) under Ar (50 sccm) and nitrogen (4~6 sccm) with an Ion Tech Merovac 450C sputtering system. $TiSi_xO_yN_z$ films were formed under Ti (200~240 W) and Si (60~80 W) under Ar (50 sccm), nitrogen (4~6 sccm) and oxygen (0.2~0.7 sccm). The deposition rate of these thin films was 12.3~15.2 nm/min.

Transmittance T% and and reflectance R% were taken from a Shimadsu UV-2501PC double-beam UV-VIS spectrometer. Thickness was measured using a Dektak 3030 surface profilometer and a n&k Technology NKT 1200 analyzer. The Ion depth profile of these thin films were analyzed by a Cameca IMS-5F secondary ion mass spectrometer (SIMS) using O_2^+ as ion source under 12.5 KV and 20,000 mass resolution power. Sheet resistances were measured using a Napson RT-7 resistance analyzer. Micrographs were taken by a Hitachi S-400 FE-SEM and a Hitachi S-6260H in-line CCFE-SEM. Atomic force microscope (AFM) used is a Digital Instruments D5000. The chemical composition of thin film surface was analyzed with a VG Microlab 310F Electron Spectroscopy for Chemical Analysis (ESCA) using Mg K_α standard source under scan 1 eV. The thermal behavior of thin film's stress was measured with a Tencor Corp. FLX-230 Stress System. The cleaning durability of

0167-9317/99/$ – see front matter
PII: S0167-9317(99)00023-4

thin films was studied at 80°C for 30 min by following four different methods and solutions, H_2SO_4-H_2O_2 (3:1) solution; NH_4OH-H_2O_2-H_2O (1:2:7) solution; DI water with a BRANSONIC 1200 ultrasonic cleaner; and OCG Microstrip 2001 solution (A mixture of N-methyl pyrrolidene and 2-(2-aminoethoxy) ethanol).

The lithographic pattern of $TiSi_xN_y$ embedded layer on SiO_2/Si substrate was carried out by a Hitachi LD-5011IA i-line (365 nm) stepper and an Anelva ILD-4100 helicon wave etcher.

3. Results and Discussion

3.1 Optical Properties

The thin film's R% and T% in 193 nm were measured, and their n and k were calculated with our modified R-T Method [7]. The R% in the range of 190~200 nm wavelength changed quite sharply, the value of R% in 193 nm is therefore not very reliable, and will effect the correct determination of n and k. The T% in the range of 190~200 nm wavelength is quite flat. The relative optical properties are shown in Table 1.

The effect of N_2 flow on n and k of $TiSi_xN_y$ was shown in Fig. 1. N_2 flow is very critical to the T%. The increasing of N_2 flow, the structure of TiN-like and Si_3N_4-like will increase, hence, the refractive index n of $TiSi_xN_y$ film will increase, and thickness of d_{180} will decrease. While the d_{180} decreased with higher N_2 flow, the T% in 193 nm increased with the thinner film. The lower the N_2 flow, the lower sheet resistance R_s will have. Under N_2 flow 4 sccm, 12.5 kΩ/square R_s was measured. The conductivity is acceptable for e-beam patterning.

When N_2 flow lower than 4 sccm, the T% at visible wavelength (488, 632.8 nm) will rise to 60~75%, no longer suitable for optical alignment. If N_2 flow was kept in 4~6 sccm, T% is 35~45%, suitable for optical alignment. When nitrogen flow is higher than 7 sccm, $TiSi_xN_y$ thin films will not have reasonable conductivity, might have charging effect during e-beam direct-write.

The effect of sputtering power of Ti target on n and k of $TiSi_xN_y$ was shown in Fig. 2. With higher power, oxidation of Ti occurred, n decreased and k increased.

The n, k, T%, and R% of $TiSi_xO_yN_z$ films could be manipulated and kept in the useful range for AttPSM. The increasing of oxygen flow, will decrease the n and k of $TiSi_xO_yN_z$ film as shown in Fig. 3. The thickness d_{180} of $TiSi_xO_yN_z$ embedded layer is in the range of 92~105 nm. Its R_s is in the range of 46~82 kΩ/square.

Compared to $TiSi_xN_y$ as shown in Table 1, $TiSi_xO_yN_z$ layer has lower values of n, k and R% in 193 nm. Another, $TiSi_xO_yN_z$ is more resistance to strong acid, higher resistivity, and higher T% at visible wavelength than $TiSi_xN_y$.

Besides the embedded layer itself, the additional phase-shift contributed from interfaces could be calculated by [1]:

$$\phi = \arg\left(\frac{2n_2^*}{n_1^* + n_2^*}\right)$$

The all interfaces were found to generate totally about -3.45° phase-shift loss from $TiSi_xN_y$ on quartz substrate and -2.78° from $TiSi_xO_yN_z$. The interface A which is between quartz and embedded layer alone contributed about 90 % of loss of phase-shift as shown in Fig. 4. The degree of loss is not critical, however, the increasing of 1~2 nm of embedded layer's thickness to compensate this loss of phase-shift is suggested.

The n, k planes of both compounds were shown in Fig. 5 which including the window suitable as embedded material in 193 nm. By controlling the sputtering conditions, the optical properties of both compounds could be kept inside this window.

3.2 Physical and Chemical Properties

MAC MXP-3 X-ray Diffractometer (XRD) was used to analyze $TiSi_xN_y$ and $TiSi_xO_yN_z$ thin films and an amorphous structure was confirmed for these films. The thermal behavior of $TiSi_xN_y$ and $TiSi_xO_yN_z$ films was illustrated in Fig. 6. The maximal tensile stresses in the range of 150~200 MPa were found during traced stress measurement by annealing in flowing nitrogen gas. The maximal tensile stresses were in acceptable range.

Table 2 listed the summaries of four different methods and solutions for testing the cleaning durability of $TiSi_xN_y$ films. The T%, R%, and thickness of these films by using the first two methods have changed greatly. ESCA analyses demonstrated the existence of Ti and TiN chemical structures in $TiSi_xN_y$ embedded material, and these structures have quite low resistance to strong acid and base solutions. Fortunately, the next two methods, DI water with ultrasonic and Microstrip solution, could be used to do the clean of $TiSi_xN_y$.

Because of expensive ArF 193 nm laser is not

Table 1. Optical properties of $TiSi_xN_y$ and $TiSi_xO_yN_z$ embedded materials

	193 nm				488 nm#	632.8 nm#
	Calculated thickness d_{180}	n, k	T%, R%	Phase shift by interfaces*	T%, R%	T%, R%
$TiSi_xN_y$	84.7 nm	2.14, 0.48	5.8%, 14.3%	-3.45°	36.1%, 22.1%	45.3%, 25.7%
$TiSi_xO_yN_z$	101.6 nm	1.95, 0.42	5.3%, 11.6%	-2.78°	40.5%, 25.2%	49.7%, 17.2%

*: Refractive index of fused silica 1.56 under 193 nm wavelength was used.
#: Wavelength for inspection and alignment.

Table 2. Cleaning durability of $TiSi_xN_y$ embedded material in 193 nm

	H_2SO_4-H_2O_2 (3:1) solution at 80℃, 30 min	NH_4OH-H_2O_2-H_2O (1:2:7) solution at 80℃, 30 min	DI water with ultrasonic at 80℃, 30 min	Microstrip 2001 solution at 80℃, 30 min
Change of T%	+38.2	+20.7	+0.3	+0.1
Change of R%	+5.9	+3.2	+0.2	+0.2
Change of thickness	-35.2 nm	-25.7 nm	-0.5 nm	-0.3 nm

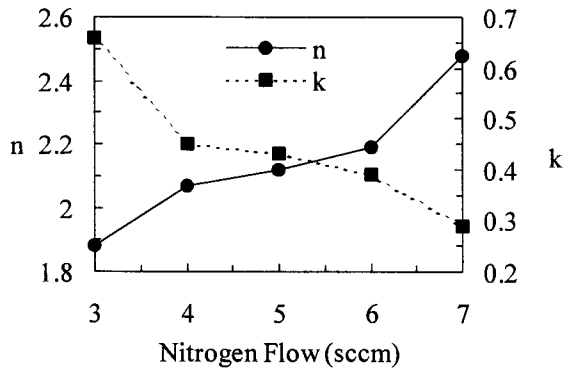

Fig. 1 The effect of N_2 flow on n and k of $TiSi_xN_y$ films under Ti 200 W, Si 60 W, and Ar 50 sccm.

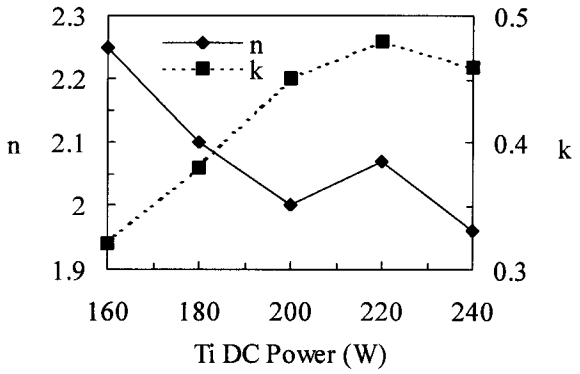

Fig. 2 The effect of power of Ti target on n and k of $TiSi_xN_y$ films under Si 80 W, Ar 50 sccm, and N_2 4 sccm.

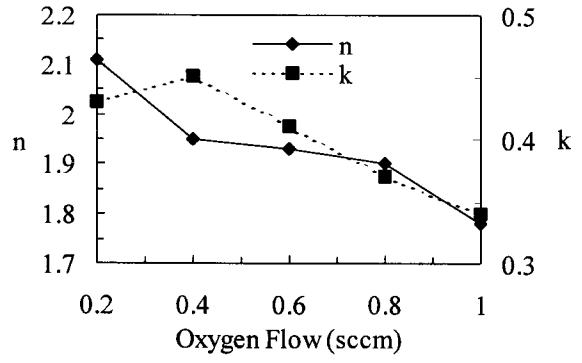

Fig. 3 The effect of oxygen flow on n and k of $TiSi_xO_yN_z$ films under Ti 180 W, Si 80 W, Ar 50 sccm, and N_2 3 sccm.

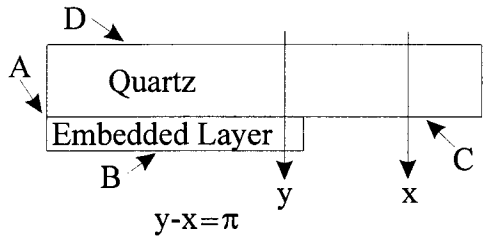

Fig. 4 Interfaces of AttPSM.

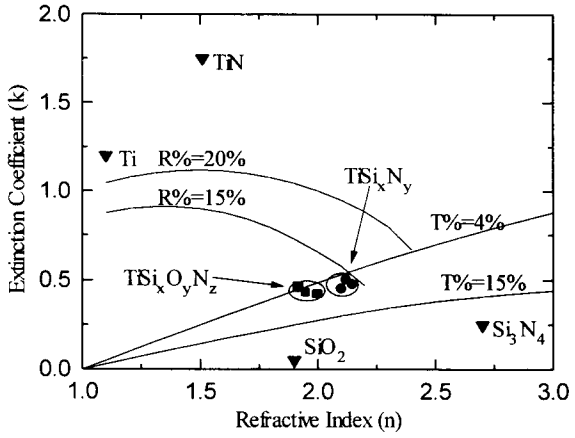

Fig. 5 n, k plane of $TiSi_xN_y$ and $TiSi_xO_yN_z$ embedded materials under 193 nm wavelength.

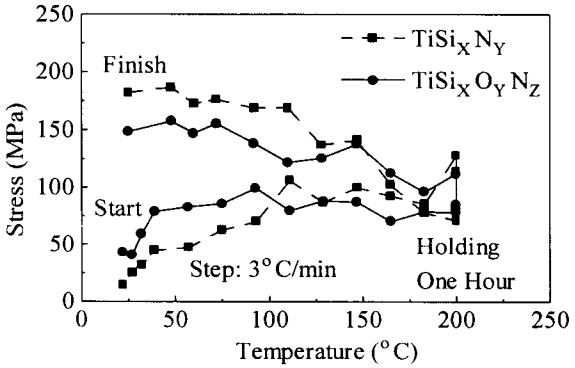

Fig. 6 The effects of temperature of $TiSi_xN_y$ and $TiSi_xO_yN_z$ films on their stresses.

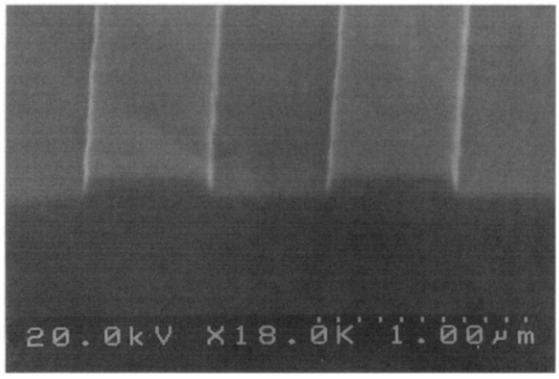

Fig. 7 SEM of a 0.6 μm line/space etched pattern of $TiSi_xN_y$ embedded layer on SiO_2/Si substrate.

available, a ~254 nm broad band deep ultraviolet light was used instead to examine the exposure durability of these thin films. Irradiation doses up to 2×10^3 J/cm^2, optical properties of $TiSi_xN_y$ thin films showed only a very slight change.

3.3 Etching Selectivity and Lithographic Pattern of $TiSi_xN_y$

The etching rate and selectivity were studied with several chlorine-based gases such as BCl_3, Cl_2, and CCl_4. The optimal conditions, BCl_3:Cl_2 = 14:70 sccm, chamber pressure 4 mtorr and RF power 1900W were used for these studies. The results indicated that the etching rate of $TiSi_xN_y$ embedded layer was 43Å/sec, etching selectivity of $TiSi_xN_y$ over resist was 2:1, over fused silica was 4.8:1.

Because 0.25 inch thickness fused silica was too thick to be placed into the chamber of helicon wave etcher, SiO_2/Si wafer was replaced as substrate for $TiSi_xN_y$ embedded layer. Fig. 7 illustrated a 0.6 μm line/space etched pattern of $TiSi_xN_y$ as embedded layer. Smaller lines did not show good results in our study so far.

4. Conclusions

$TiSi_xN_y$ and $TiSi_xO_yN_z$ thin films have the potential as good embedded materials for AttPSM in 193 nm. By controlling the sputtering conditions, a wide range of optical properties of $TiSi_xN_y$ and $TiSi_xO_yN_z$ films can be deposited.

References:

[1] B. W. Smith et al., Microelectronic Engineering, ***35***, p. 201 (1997).
[2] U. Ushioda, Y. Seki, K. Maeda, T. Ohfuji and H. Tanabe, Jpn. J. Appl. Phys., Part 1, ***35(12B)***, p. 6356 (1996).
[3] T. Matsuo, K. Ohkubo, T. Haraguchi and K. Ueyama, Proc. SPIE, Vol. 3096, pp. 354-361 (1997).
[4] Y. Seki et al., SPIE, ***3096***, p. 286 (1997).
[5] W. A. Loong, T. C. Chen and J. C. Tseng, Microelectronic Engineering, ***30***, p. 157 (1996).
[6] W. A. Loong, T. C. Chen S. L. Shy, J. C. Tseng and R. J. Lin, SPIE, ***2726***, p. 524 (1996).
[7] W. A. Loong, C. W. Chen, Y. H. Chang, C. M. Lin, Z. Cui and C. A. Lung, Microelectronic Engineering, ***41/42***, p. 125 (1998).